Article 3.

INFLUENCE OF SOOT CARBON ON THE SOIL-AIR PARTITIONING OF POLYCYCLIC AROMATIC HYDROCARBONS

Sandra Ribes [1], Barend van Drooge [1], Jordi Dachs [1], Ørjan Gustafsson [2], Joan O. Grimalt [1]

[1] Department of Environmental Chemistry, ICER-CSIC, Barcelona, Catalonia, Spain
[2] Institute of Applied Environmental Research, Stockholm University, Stockholm, Sweden

Environmental Science & Technology, 2003, 37, 2675-2680

Environ. Sci. Technol. **2003**, *37*, 2675−2680

Influence of Soot Carbon on the Soil−Air Partitioning of Polycyclic Aromatic Hydrocarbons

SANDRA RIBES,† BAREND VAN DROOGE,† JORDI DACHS,*,† ØRJAN GUSTAFSSON,‡ AND JOAN O. GRIMALT†

Department of Environmental Chemistry (ICER-CSIC), Jordi Girona 18-26, Barcelona 08034, Catalonia, Spain, and Institute of Applied Environmental Research, Stockholm University, Stockholm, Sweden

Soil−air partitioning is one of the key processes controlling the regional and global cycling and storage of polycyclic aromatic hydrocarbons (PAHs). However, the specific processes dominating the partitioning of PAHs between these two environmental compartments still need to be elucidated. Stable and distinct atmospheric conditions paralleling different soil properties are found at Tenerife island (28°18′N, 16°29′W), which is located in permanent inversion layer conditions, and they provide interesting model cases for the study of air−soil partitioning. Analysis of phenanthrene, pyrene, fluoranthene, and chrysene showed concentrations 4- to 10-fold higher below than above the inversion layer. Similarly, soil total organic carbon (TOC) and black carbon (BC) were 11 and 3 times higher, respectively, below the inversion layer than above. The octanol−air partition coefficient (K_{OA}) derived model provides a good description of PAH soil−air partitioning coefficients (K_P) below the inversion layer but underpredicts them in the area dominated by deposition of long-range transported aerosols without inputs of organic matter from local vegetation. Inclusion of soot carbon in the soil−air partitioning model results in good agreement between predicted and measured K_P in this area but in overpredicted K_P values for the soils under the vegetation cover, which shows that the influence of soil soot carbon on PAH air−soil partitioning depends on its abundance relative to soil organic carbon. Absorption into organic matter is the dominant process in soils containing high organic carbon concentrations, whereas adsorption onto soot carbon becomes relevant in soils with low organic carbon and high soot content.

Introduction

Soil is the primary terrestrial reservoir of persistent organic pollutants (POPs) such as PAHs (*1*−*7*), and the atmosphere is their main transport vector (*8*−*11*). Soil−air exchange is therefore a key process governing the environmental fate of these compounds on a regional and global scale. Air to soil transport may occur through dry deposition of aerosols, wet deposition, or sorption to soil constituents (*12*). Soil to air diffusion is driven by the chemical potential gradient between the soil and the atmosphere. In most cases it is not clear whether soil−air partitioning is dominated by adsorption onto soil surface or absorption into the bulk soil constituents (*13*). Sorption is also dependent on temperature, relative humidity (*14*), and other soil properties such as specific surface area, particle diameter, and clay mineralogy (*15*). Nevertheless, most studies have concluded that sorption to soils is primarily controlled by partitioning into organic matter (*12*−*13*, *16*−*17*).

At equilibrium, the POP soil−air partition coefficients (K_P) for a wide range of persistent organic pollutants such as polychlorinated biphenyls are predicted from the octanol−air partition coefficients (K_{OA}; *18*−*19*). However, these studies have been focused in soils with high concentrations of organic matter, and the predictive capability of this model is limited for PAHs. The chemical and physical heterogeneity of soil organic matter and soil constituents such as soot carbon are likely additional structural parameters that influence POP sorption (*13*, *15*, *17*, *20*−*21*) but their significance is not properly evaluated with the K_{OA} model.

Soils contain different forms of carbonaceous materials. Black carbon (BC), produced by the incomplete combustion of fossil fuels and from vegetation fires, occurs ubiquitously. It can account for about half of the total organic carbon in certain soils (*22*−*23*). Structurally, BC may be essentially differentiated between soot carbon (small particle size; SC) and char/charcoal. The former originate during the condensation of hot combustion gases involving free radical reactions of acetylene species leading into PAH, macro PAH, and SC. Conversely, charcoal originates from incomplete combustion of plant tissues and diagenesis (*24*−*25*) and always contains a core of unburned biomass material (with cell structures frequently discernible).

During the past few years, the study of SC as a strong sorption matrix has received increasing attention (*22*−*32*). Adsorption onto SC has been shown to affect significantly the overall PAH sorption to sediments and aerosols (*27*−*34*) but to date its role in the soil−air PAH partitioning has not been considered. The influence of other forms of condensed organic carbon such as char/charcoal BC on air−soil partitioning also remains to be investigated. The present study is therefore devoted to assessing the sorption mechanisms driving soil−air partitioning of PAHs through the evaluation of soil−air partition models based on the octanol−air (K_{OA}) and soot−air partition coefficients (K_{SA}).

Experimental Section

Sampling. Soil samples were taken at different altitudes between 10 and 3400 m above sea level (masl) on the northern side of Tenerife Island (28°18′N, 16°29′W) which is situated in the subtropical Atlantic ocean. Soils between 10 and 2500 masl were collected with a soil corer (Lancaster University), whereas the upper soils (very stony) were sampled with a small shovel and sifted through a 500-μm sieve.

Air samples were collected at Punta del Hidalgo (47 masl) and Izaña (2367 masl). Air volumes of 80 m^3 were collected with a high-volume sampler (MCV S. A., Collbató, Catalonia, Spain) for a period of time ranging from 4 to 8 h. Aerosols were collected on glass fiber filters (GFF, Whatman International Ltd, Maidstone, England; 20.3 × 25.4 cm; 1.0 μm pore size), and gas-phase PAHs were retained on two polyurethane foam (PUF) plugs which had been previously cleaned by Soxhlet extraction with *n*-hexane. Both soil and PUFs were wrapped in aluminum foil, packed into heat-

* Corresponding author phone: +349334006100; fax +34932045904; e-mail: jdmqam@iiqab.csic.es.
† Department of Environmental Chemistry (ICER-CSIC).
‡ Stockholm University.

10.1021/es0201449 CCC: $25.00
Published on Web 05/10/2003

sealed polyester bags (Kapak corporation, Minneapolis, MN) and stored at 4 °C until analysis.

Extraction and Fractionation of PAHs in Soils. About 50 g of fresh soil was mixed with 25−50 g of anhydrous sodium sulfate for water removal. The mixtures were introduced into Whatman Soxhlet cellulose thimbles, spiked with d_{10}-benzo-[*a*]pyrene and d_{12}-benzo[*ghi*]perylene (Cambridge Isotope Lab.), and extracted with hexane/dichloromethane (4:1) for 18 h. All extracts were first concentrated by rotary vacuum evaporation to 3−5 mL and subsequently further dehydrated by elution through sodium sulfate. After rotary vacuum evaporation to ~0.5 mL, the extracts were fractionated by column chromatography using 2 g of neutral aluminum oxide. PAHs were obtained by elution with 10 mL of hexane/dichloromethane (1:2). Subsequently, the eluate was hydrolyzed overnight with KOH in methanol to remove aliphatic ester interferences. Neutral compounds were recovered with *n*-hexane and fractionated again by adsorption chromatography with aluminum oxide (2 g). After elution with hexane/dichloromethane (1:2), the PAH fraction was concentrated to 50 μL in isooctane by rotary vacuum evaporation followed by a gentle stream of purified N_2.

Extraction and Fractionation of Gas-Phase PAHs. PUFs were spiked with d_{10}-anthracene, d_{10}-benzo[*a*]pyrene, and d_{12}-benzo[*ghi*]perylene immediately after sampling to check for losses during transport and analysis. The two plugs were Soxhlet extracted in *n*-hexane for 24 h. The extracts were vacuum evaporated until 1 mL. Samples and blanks were cleaned up by adsorption on 2 g of neutral aluminum oxide. PAHs were obtained by elution with 7 mL of hexane/dichloromethane (1:2). The collected fraction was vacuum evaporated to 1 mL and then further concentrated to 50 μL under a gentle stream of nitrogen.

Instrumental Analysis. The internal standards tetrachloronaphthalene and octachloronaphthalene (L. D. Ehrenstorfer) were added to the vials prior to injection. The samples were injected into a gas chromatograph equipped with a mass selective detector (Fisons 8000 Series, Mass Selective Detector 800 Series). A fused silica capillary column (HP-5: 30 m long, 0.25 mm i.d, 0.25 μm film thickness) was used. The oven temperature program started at 90 °C (1 min hold), followed by a 4°/min ramp up to 300 °C (15 min hold). Injector and detector temperatures were 280 and 350 °C, respectively. Helium was used as carrier gas (3 mL/min). The molecular weight mass fragments of the individual PAHs were used for identification and quantification. Quantification was performed by combination of the external standard (EPA, Mix 9, L. D. Ehrenstorfer) and retention index methods. Calibration curves (detector response vs amount injected) were performed for each PAH. The range of linearity of the detector was evaluated from the curves generated by representation of detector signal/amount injected vs amount injected. All measurements were performed in the ranges of linearity found for each compound. The quantitative data were corrected for surrogate recoveries.

Total Organic Content (TOC) and Black Carbon (BC). TOC was measured by flash combustion at 1025 °C followed by thermal conductivity detection in a CHNS elemental analyzer EA1108 (detection limit 0.1%). BC was determined by the chemothermal oxidation (CTO) method (*24, 27*) (detection limit 4 μg of C). In the present paper BC refers to the measurements with this CTO method, and SC refers to soot carbon (as defined above) which in some cases may be similar to the BC measurements.

Quality Control and Assurance. Field blanks were inserted between the air samples for monitoring for possible contamination during transport and processing. They were treated and analyzed as regular samples and constituted about 30% of total samples analyzed. Fluoranthene and pyrene concentrations in blanks were in the range of 0.2−6% of sample concentration, whereas blank phenanthrene and chrysene + triphenylene concentrations were in the range of 1.6−13% of sample concentrations. For each batch of samples and blanks, sample concentrations were handled after subtraction of blank levels. Average recoveries of d_{10}-anthracene and d_{10}-pyrene for gas-phase PAH were 82 and 107%, respectively. Detection limits (determined as three times the standard deviation of the chromatographic noise near the PAH peaks) ranged between 0.025 pg/m^3 and 2 pg/m^3. PUF breakthrough was determined by injection of a mixture of phenanthrene, fluoranthene, pyrene, and chrysene + triphenylene into the first PUF plug before sampling. Replication of this test on four occasions did not show any traces of pyrene and chrysene + triphenylene in the second PUF plug and the levels of phenanthrene and fluoranthene were 7 and 6% of those in the first plug, respectively.

Negative bias in gas-phase determination may occur by PAH adsorption to filters during sampling. A recent rigorous examination of this sampling artifact showed that for sufficient sampling volume the measured gas-phase concentrations of the more volatile PAHs are close to the real values (*35*). In the present study, the measured sample volumes were 80 m^3 which corresponds to errors lower than 10% for the gas-phase concentrations of the compounds of interest.

Analysis of procedural blanks was performed with each set of nine soil samples to check for possible impurities. Replicate analysis gave dispersions lower than 15% and detection limits between 2 and 8 pg/g for soil PAH concentrations. Recoveries of d_{10}-benzo[*a*]pyrene and d_{12}-benzo[*ghi*]perylene spiked in soils averaged 66 and 82%, respectively.

The CTO method has been thoroughly tested with a wide range of potentially interfering substances and with ancillary environmental data (*24, 27*). Although there may be limitations in high-organic/low-BC matrices such as peat and plankton, the method has been demonstrated to return geochemically and isotopically consistent results for coastal sediments and aerosol particles (*24, 27, 36, 37*).

Results and Discussion

Atmospheric Conditions. The volcanic mountain system in the subtropical Atlantic Ocean is characterized by a yearly stable temperature inversion that separates air masses of lower altitude (0−1000 masl) from the free troposphere (above 1800 m). These atmospheric conditions result from the descent branch of the Hadley cell at this latitude. On the northern side of Tenerife, the atmospheric inversion layer is further enforced by a strong humidity inversion due to the influence of a wet northeastern air mass (trade winds). The combination of these two factors leads to the formation of low stratus clouds and the stabilization of two independent air masses year-round. This atmospheric structure has led to the formation of two different soil types. Entisoils predominate above the inversion layer constituting practically not-developed soils with low TOC and water content. Andisoils are the dominant form below the inversion layer (*38*).

The present study is focused in these two well-defined environments, below (0−800 masl) and above (more than 1800 masl) the inversion layer, because the atmospheric conditions are more stable and better characterized at these two altitude ranges.

Occurrence of Soil and Gas-Phase PAHs. The major gas-phase PAHs encompass naphthalene, fluorene, phenanthrene, fluoranthene, and pyrene (*39−40*). Among these, the present study is focused on the compounds currently found in higher concentration in soils, e.g., phenanthrene, fluoranthene, and pyrene. For comparison, chrysene + triphenylene is also considered. Furthermore, K_{OA} and K_{SA} values for these compounds are known (*31, 41*).

TABLE 1. Mean and Range (in parentheses) Soil and Gas-Phase PAH Concentrations, Soil Total Organic Carbon (f_{TOC}), and Soil Black Carbon (f_{BC}) Concentrations Below (BIL) and Above (AIL) the Atmospheric Inversion Layer

	BIL (0−800 masl)		AIL (1800−3400 masl)	
	soil[a] (n = 12)	gas phase[b] (n = 4)	soil (n = 26)	gas phase (n = 12)
sampling mean temperature (°C)	26	20	16	16
phenantrene (Phe)	0.81 (0.01−3.0)	980 (270−6000)	0.97 (0.03−6.8)	63 (35−150)
fluoranthene (Fla)	120 (0.03−1400)	830 (37−3600)	7.2 (0.17−130)	24 (2.9−25)
pyrene (Pyr)	10 (0.01−75)	350 (28−1400)	2.4 (0.10−23)	23 (1.4−21)
chrysene + triphenylene (C+T)	83 (0.05−1000)	54 (16−70)	24 (0.02−500)	16 (3.5−25)
f_{BC} ($\times 10^3$ g/g dw)	0.76 (0.19−2.4)		0.25 (0.06−0.91)	
predicted f_{sc} ($\times 10^3$ g/g dw)[c]	0.03 (0.01−0.09)		0.01 (0.002−0.04)	
f_{TOC} ($\times 10^3$ g/g dw)	29 (3.3−74)		2.6 (0.46−15)	
f_{BC}/f_{TOC}	0.03 (0.03−0.06)		0.10 (0.06−0.13)	

[a] Results for PAHs are given in ng/g dry weight. [b] Results for PAHs are given in pg/m³. [c] Assuming SC = 0.04 · BC (*43*).

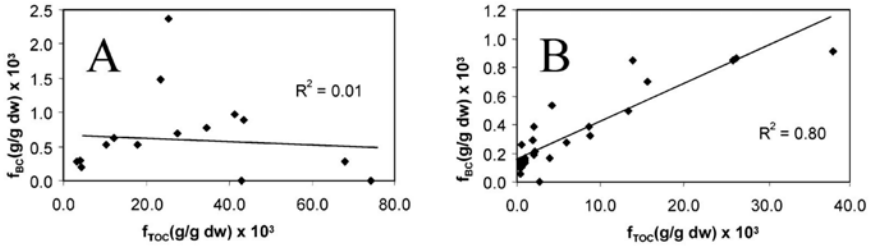

FIGURE 1. Correlation between BC concentrations and TOC in soils below (A) and above (B) Tenerife inversion layer.

Gas-phase PAH concentrations in the two vertically stratified air masses of the island are higher below the inversion layer (0−800 masl) than above it (1800−3400 masl). Measurements at Punta del Hidalgo (below inversion layer) encompass 351−11 070 pg/m³ whereas at Izaña (above inversion layer) they range between 45 and 221 pg/m³. (Table 1). The concentrations of these compounds within the inversion layer are similar to those encountered in coastal atmospheres and high-altitude sites (*31, 40*) and between 10 and 50 times lower than those found in urban areas (*31, 39*).

The differences between the two Tenerife soils are also reflected in PAH concentrations being higher below (0.1−2474 ng/g dw) than above the atmospheric inversion layer (0.3−660 ng/g dw) (Table 1). Soil PAH concentrations below the inversion layer are similar to the concentrations encountered in rural sites (*41−42*).

TOC and BC. TOC and BC concentrations, f_{TOC} and f_{BC}, respectively, are 10- to 3-fold higher, respectively, below the atmospheric inversion layer than above (Table 1). At lower altitudes there is higher variability and no significant correlation between f_{TOC} and f_{BC}. Conversely, above the inversion layer, f_{TOC} and f_{BC} show a positive significant correlation explaining 80% of the observed variability (Figure 1). This difference is consistent with the two different soils distributed vertically in the Teide Mountain.

The f_{BC}/f_{TOC} mean ratios of 0.03 and 0.10 are found below and above the inversion layer, respectively. The latter are close to those observed in aerosols of semi-rural areas (*31, 37, 44*) suggesting that deposition of aerosols may be a major BC source above the inversion layer (*45*). Thus, in these soils, BC may be predominantly SC. A correlation between f_{BC} and f_{TOC} is also commonly observed in atmospheric aerosols (*31, 44−46*) giving further support to this interpretation.

Conversely, the f_{BC}/f_{TOC} ratios below the inversion layer are in agreement with those found in soils under vegetation (0.01−0.07; *31, 37*) involving higher humic material content, and, to a lesser extent, higher char/charcoal BC. In any case, the anthropogenic activity below the inversion layer also generates SC, contributing to total BC. Fresh organic matter is therefore expected to predominate below the inversion layer and the measured BC values may contain a significant fraction of charcoal besides the anthropogenic SC. Indeed, there is no generally accepted analytical protocol and terminology for BC determination in soils. Different optical, chemical, and thermal methods are currently used. A recent comparative study (*37, 43*) for soils showed that the values measured had a wide range of variability, suggesting that the BC concept depends to a certain extent on the determination method.

Soil−Air Partitioning. The soil−air partition coefficient K_P (L/kg) is given by

$$K_p = C_S/C_G \quad (1)$$

where C_S is the individual PAH concentration in soil (pg/kg soil dry-weight) and C_G is the individual PAH concentration in the gas phase (pg/L sampled air).

Sorption to Organic Matter. The octanol−air partition coefficients have recently been useful to predict K_P values for a wide range of POPs (*18−19, 41, 47, 48*). This model is consistent with absorption into organic matter as the dominant sorption mechanism. K_P values are predicted from K_{oa} according to the following equation:

$$K_p = f_{OM}\,(\zeta_{OCT}/\zeta_{OM})(MW_{OCT}/MW_{OM}\delta_{OCT})\,K_{oa} \quad (2)$$

where f_{OM} is the fraction of organic matter in the soil (g/g soil dw), and ζ_{OCT} and ζ_{OM} are the activity coefficients of the individual PAH in octanol and soil organic matter, respectively. MW_{OCT} and MW_{OM} are the molecular weights of octanol (130 g/mol) and organic matter, respectively, and δ_{OCT} is the octanol density (0.820 kg/L, 20 °C).

Prediction of K_p values from eq 2 is limited by the lack of knowledge on ζ_{OM}, ζ_{OCT}, and MW_{OM}. Usually, the following

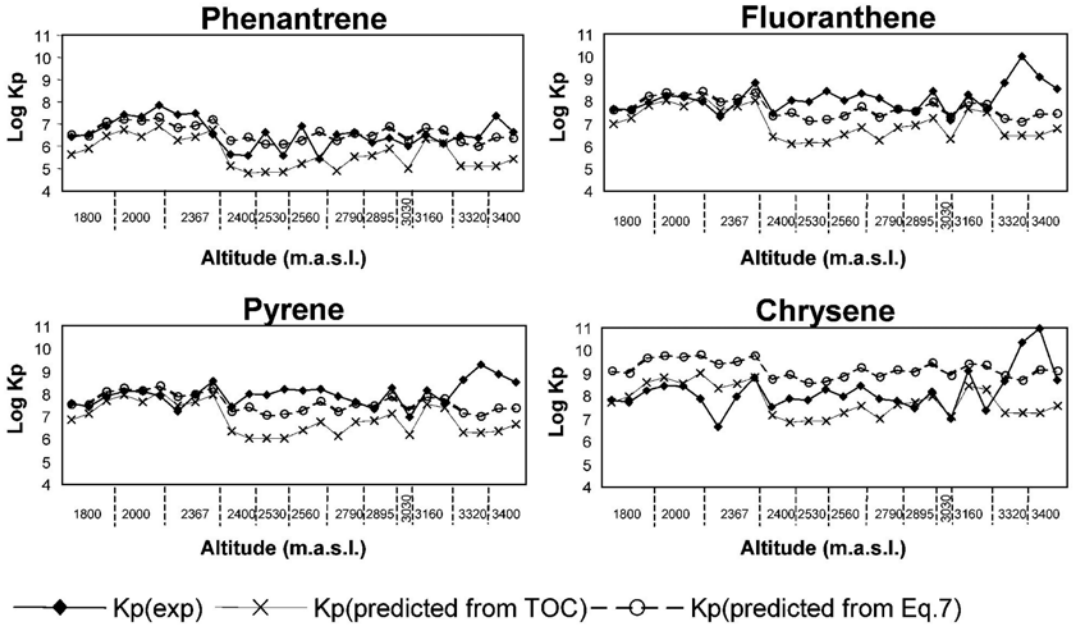

FIGURE 2. Experimental and predicted log-transformed K_p values for the soil samples collected above the inversion layer. Predicted K_p values have been estimated from TOC and eq 7 (applying SC = BC). X axis indicates altitude in meters above sea level (masl).

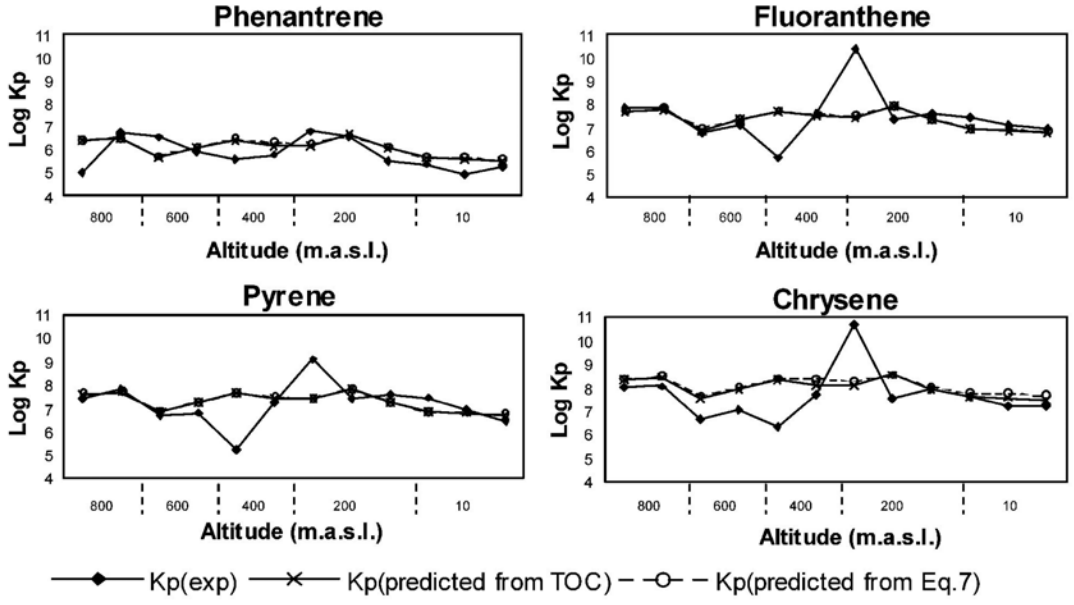

FIGURE 3. Experimental and predicted log-transformed K_p values for the soil samples collected below the inversion layer. Predicted K_p values have been estimated from TOC and eq 7 (applying SC = 0.04 BC). X axis indicates altitude in meters above sea level (masl).

assumptions are considered (*31*, *47*):

$$f_{OM} = 1.5\ f_{TOC}$$

$$(\zeta_{OCT}/\zeta_{OM})(MW_{OCT}/MW_{OM}) = 1$$

where f_{TOC} is the fraction of total organic carbon (g/g dw).

Then, K_P is given by

$$K_p = 1.5\ (f_{TOC}/\delta_{OCT})\ K_{oa} \qquad (3)$$

This absorption model has already been applied to predict K_p values for PAH gas−particle partitioning (*18*, *31*, *47*). Therefore, the K_{oa} absorption model requires knowledge of only two easily measurable parameters, K_{oa} and f_{TOC}. In the

TABLE 2. PAH Physical–Chemical Parameters and Partition Coefficients at 298K

	Log K_{OA}	Log K_{OW}[c]	Log K_{SW} (L/kg)	Log K_{SA}[f] (L/kg)
Phe	7.45[a]	4.57	6.22[d]	9.13
Fla	8.80[a]	5.22	6.96[e]	10.58
Pyr	8.43[a]	5.18	6.79[d]	10.23
C + T	10.40[b]	5.86	8.18[e]	12.27

[a] From ref (*41*). [b] Estimated from $K_{OA} = K_{OW}/H'$. [c] From ref (*49*). [d] From ref (*29*). [e] From ref (*32*). [f] Estimated from $K_{SA} = K_{SW}/H'$.

present study the K_{OA} values reported elsewhere for phenanthrene, pyrene, and fluoranthene have been used (*41*), whereas for chrysene, K_{OA} was estimated from the octanol–water partition coefficient (K_{OW}) and the dimensionless Henry's law constant (H'). The influence of temperature on K_{OA} and H has been taken into account following the procedure described elsewhere (*31*, *47*–*48*).

Figures 2 and 3 show the measured and predicted K_p values from eq 3 for samples above and below the inversion layer, respectively. Above the inversion layer, the measured K_P is underpredicted by 1 order of magnitude. A paired t test has confirmed the significance of the differences between predicted and measured K_P values ($p < 0.05$). Conversely, below the inversion layer, predictions of K_P from K_{OA} significantly agree with the measured K_P values.

Soot Carbon Adsorption Model. The high PAH affinity for SC in sediments and aerosols has been demonstrated recently (*27*–*34*). K_p values can therefore be estimated by a soot-inclusive gas–particle partitioning model (*31*)

$$K_P = 1.5\ (f_{TOC}/\delta_{OCT})\ K_{OA} + f_{SC}\ K_{SA} \quad (4)$$

where K_{SA} and f_{SC} are the soot–air partition coefficient (L kg^{-1}) and the fraction of soot carbon in the soil (g SC/g dw), respectively.

Because of the lack of experimental K_{SA} values, these are estimated from the soot–water partition coefficient (K_{SW}, L kg^{-1}) by

$$K_{SA} = K_{SW}/H' \quad (5)$$

In the present study, the K_{SW} values reported by Gustafsson (*29*) and Jonker and Koelmans (*32*) are used.

On the other hand, there is uncertainty with the estimation of f_{SC} from BC measurements for soils rich in organic matter (*24*, *43*), as the latter may include the contribution of different forms of condensed carbon such as SC and charcoal. Studies involving thermal oxidation with demineralization and hydrolysis for the specific measurement of SC showed that the f_{SC}/f_{BC} ratio in soils with high f_{TOC} (0.025–0.070 g/g dw; *43*) is fairly constant and about 0.04 in most cases. This suggests that a tentative general assumption of a f_{SC}/f_{BC} ratio equal to 0.04 may be considered for these soil types. However, this may not be true for soils with low f_{TOC} concentrations as those above the inversion layer. Recent work by Gustafsson et al. (*24*) has shown that in low f_{TOC} soils the chemothermal oxidation method provides direct f_{SC} values. In this respect, the linear correlation between f_{BC} and f_{TOC} above the inversion layer and the high f_{BC}/f_{TOC} ratios in these soils suggest that BC may be predominantly SC for these samples. In the present study, the soot-inclusive model is tested under two different potential scenarios: the first, that BC measurements are representative of real SC concentrations ($f_{SC} = f_{BC}$), and, second, that f_{SC} is only 4% of f_{BC} ($f_{SC} = 0.04\ f_{BC}$).

The K_P values predicted with the SC model outlined in eq 4 are shown in Figures 2 and 3. Above the inversion layer, the soot-inclusive model using the measured BC concentrations predicts the measured K_P values within a factor of 3 (see Table 3) and differences between measured and predicted K_P are not significant for most PAHs. This provides evidence that adsorption onto soil soot carbon controls the soil–air partitioning of PAHs above the atmospheric inversion layer. However, predictions of K_P using the estimated SC concentrations from SC/BC = 0.04 underpredict the measured K_P values. Therefore, for the soils above the inversion layer with low TOC concentrations, the measured BC concentrations are representative of the real soot carbon content. Conversely, below the inversion layer, the soot-inclusive model using the BC concentrations does not improve the model predictions — on the contrary, it overpredicts the measured K_P values. However, in this case, the use of estimated SC (SC/BC = 0.04) also provides accurate predictions, even though in this case it has virtually no influence on the predicted K_P because of the low SC concentrations. Therefore, below the inversion layer, the high concentration of organic carbon dominates the soil–air partitioning of PAHs. Another reason for the apparent lack of influence of SC in rich soils may be that the high concentrations of fresh organic matter may hinder the soot carbon fraction which may not be available to gas-phase PAHs.

Dominant Soil–Air Partitioning Mechanism. As discussed above, the dominant mechanism of PAH soil–air partitioning depends on soil characteristics. Having in mind the assumptions reported above for molecular mass of organic matter and activity coefficients in octanol and organic matter, the ratio $f_{SC}K_{SA}\delta_{OCT}/f_{OM}K_{OA}$ has been proposed to determine the dominant gas-particle partitioning (*31*). Absorption into organic matter is the dominant sorption mechanism when f_{OC} is more than 2 orders of magnitude higher than f_{SC}. Indeed, this is the case of the soils located at low altitudes of Tenerife Island (see Table 1).

Therefore, below the atmospheric inversion layer, the high concentrations of soil organic carbon dominate the soil–air partitioning of PAHs. This may be true also in those areas with abundant vegetation or rich soils with high f_{OC} values. Furthermore, high concentrations of organic matter may cover the soot carbon content in soils and therefore it may not be always available to gas-phase compounds. In contrast, the soils situated above the inversion layer correspond to a $f_{SC}K_{SA}\delta_{OCT}/f_{OM}K_{OA}$ ratio higher than one due to relatively high f_{SC} values and therefore adsorption to soil SC is the dominant

TABLE 3. Statistical Comparison of Measured and Predicted K_p Values below (BIL) and above (AIL) the Inversion Layer at Tenerife

Compared Means[a]	mean difference (measured Log K_P − predicted Log K_P)		p-value	
Log K_p (exp) vs.	BIL	AIL	BIL	AIL
Log K_p (predicted from eq 3)	−0.07	1.03	0.63	<0.00001
Log K_p (predicted from eq 4[b])	−0.66	0.26	<0.0001	0.03
Log K_p (predicted from eq 4[c])	−0.12	0.93	0.39	<0.0001

[a] Compared means correspond to all the available data from Phe, Fla, Pyr, and C + T. The t test for paired samples was conducted at $p < 0.05$ (95% confidence level). [b] SC = 0.04 · BC. [c] SC = BC.

process. Generalizing, this will be the scenario also for soils poor in organic matter that are receptive of deposited aerosols.

Literature Cited

(1) Guggenberg, G.; Pichler, M.; Hartmann, R.; Zech, W. *Z. Pflanzenernähr. Bodenk.* **1996**, *159*, 563−573.
(2) Jones, K. C.; Stratford, J. A.; Waterhouse, K. S.; Vogt, N. B. *Environ. Sci. Technol.* **1989**, *23*, 540−550.
(3) Ribes, A.; Grimalt, J. O.; Torres-Garcia, C. J.; Cuevas, E. *Environ. Sci. Technol.* **2002**, *36*, 1879−1885.
(4) Meijer, S. N.; Steinnes, E.; Ockenden, W. A.; Jones, K. C. *Environ. Sci. Technol.* **2002**, *36*, 2146−2153.
(5) Jones, K. C.; Stratford, J. A.; Tidridge, P.; Waterhouse, K. S.; Johnston, A. E. *Environ. Pollut.* **1989**, *56*, 337−351.
(6) Wilcke, W.; Zech, W.; Kobza, J. *Environ. Pollut.* **1996**, *92*, 307−313.
(7) Wilcke, W.; Müller, S.; Kanchanakool, N.; Niamskul, Ch.; Zech, W. *Geoderma* **1999**, *91*, 297−309.
(8) Hoff, R. M.; Muir, D. C. G.; Grift, N. P. *Environ. Sci. Technol.* **1992**, *26*, 276−283.
(9) Larsson, P.; Okla, L. *Atmos. Environ.* **1989**, *23*, 1699−1711.
(10) Van Drooge, B.; Grimalt, J. O.; Torres-Garcia C. J.; Cuevas, E. *Environ. Sci. Technol.* **2002**, *36*, 1155−1161.
(11) Pacyna, J. M.; Oehme, M. *Atmos. Environ.* **1988**, *22*, 243−257.
(12) Cousins, I. T.; Beck, A. J.; Jones, K. C. *Sci. Total Environ.* **1999**, *228*, 5−24.
(13) Pignatello, J. J. *Adv. Colloid Interface Sci.* **1998**, *76−77*, 445−467.
(14) Hippelein, M.; McLachlan, M. S. *Environ. Sci. Technol.* **2000**, *34*, 3521−3526.
(15) Ahmad, R.; Kookana, R. S.; Alston, A. M.; Skjemstad, J. O. *Environ. Sci. Technol.* **2001**, *35*, 878−884.
(16) Weber, W. J.; Smith, E. H. *Environ. Sci. Technol.* **1987**, *21*, 1040−1050.
(17) Xing, B.; Pignatello, J. J.; Gigliotti, B. *Environ. Sci. Technol.* **1996**, *31*, 1578−1579.
(18) Harner, T.; Bidleman, T. F.; Jantunen, L. M. M.; Mackay, D. *Environ. Toxicol. Chem.* **2001**, *20*, 1612−1621.
(19) Finizio, A.; Mackay, D.; Bidleman, T.; Harner, T. *Atmos. Environ.* **1997**, *31*, 2289−2296.
(20) Garbarini, D. R.; Lion, L. W. *Environ. Sci. Technol.* **1986**, *20*, 1263−1269.
(21) Weber, W. J., Jr; Huang, W. *Environ. Sci. Technol.* **1996**, *30*, 881−888.
(22) Skjemstad, J. O.; Clarke, P.; Taylor, J. A.; Oades, J. M.; McClure, S. G. *Aust. J. Soil Res.* **1996**, *34*, 251−271.
(23) Schmidt, M. W. I.; Knicker, H.; Hatcher, P. G.; Kögel-Knaber, I. *Eur. J. Soil Sci.* **1999**, *50*, 351−365.
(24) Gustafsson, Ø.; Bucheli, T. D.; Kukulska, Z.; Andersson, M.; Largeau, C.; Rouzaud, J.-N.; Reddy, C. M.; Eglinton, T. I. *Global Biogeochem. Cycles* **2001**, *15*, 881−890.
(25) Schmidt, M. W. I.; Noack, A. G. *Global Biogeochem. Cycles* **2000**, *14*, 777−793.
(26) McGroddy, S. E.; Farrington, J. W. *Environ. Sci. Technol.* **1995**, *29*, 1542−1550.
(27) Gustafsson, Ø.; Haghseta, F.; Chan, C.; Macfarlane, J.; Gschwend, P. M. *Environ. Sci. Technol.* **1997**, *31*, 203−209.
(28) Gustafsson, Ø.; Gschwend, P. M. In *Molecular Markers in Environmental Geochemistry*; Eganhouse, R. P., Ed.; ACS Symposium Series 671; American Chemical Society: Washington, DC, 1997.
(29) Bucheli, T. D.; Gustafsson, Ø. *Environ. Sci. Technol.* **2000**, *34*, 5144−5151.
(30) Simó, R.; Grimalt, J. O.; Albaigés, J. *Environ. Sci. Technol.* **1997**, *31*, 2697−2700.
(31) Dachs, J.; Eisenreich, S. J. *Environ. Sci. Technol.* **2000**, *34*, 3690−3697.
(32) Jonker, M. T. O.; Koelmans, A. A. *Environ. Sci. Technol.* **2001**, *35*, 3742−3748.
(33) Naes, K.; Axelman, J.; Näf, C.; Broman, D. *Environ. Sci. Technol.* **1998**, *32*, 1786−1792.
(34) Accardi-Dey, A.; Gschwend, P. M. *Environ. Sci. Technol.* **2002**, *36*, 21−29.
(35) Mader, B. T.; Pankow, J. F. *Environ. Sci. Technol.* **2001**, *35*, 3422−3432.
(36) Reddy, C. M.; Pearson, A.; Xu, L.; Mcnichol, A. P.; Benner, B. A., Jr.; Klouda, G. A.; Currie, L. A.; Eglinton, T. I. *Environ. Sci. Technol.* **2002**, *36*, 1774−1782.
(37) Currie, L. A.; Benner, B. A., Jr.; Kessler, J. D.; Klinedinst, D. B.; Klouda, G. A.; Marolf, J. V.; Slater, J. F.; Wise, S. A.; Cachier, H.; Cary, R.; Chow, J. C.; Watson, J.; Druffel, E. R. M.; Masiello, C. A.; Eglinton, T. I.; Pearson, A.; Reddy, C. M.; Gustafsson, Ø.; Quinn, J. G.; Hartmann, P. C.; Hedges, J. I.; Prentice, K. M.; Kirchstetter, T. M.; Novakov, T.; Puxbaum, H.; Schmid, H. *J. Res. Natl. Inst. Stand. Technol.* **2002**, *107*, 279−298.
(38) Fernández-Caldas, E.; Tejedor-Salguero, M.; Quantin, P. *Suelos de Regiones Volcánicas. Tenerife. Vol IV.* Colección Viera y Clavijo. 1982.
(39) Rosell, A.; Grimalt, J. O.; Rosell, M. G.; Guardino, X.; Albaiges, J. *Fresenius' J. Anal. Chem.* **1991**, *339*, 689−698.
(40) Fernandez, P.; Grimalt, J. O.; Vilanova, R. M. *Environ. Sci. Technol.* **2002**, *36*, 1162−1168.
(41) Harner, T.; Bidleman, T. F. *J. Chem. Eng. Data* **1996**, *41*, 895−899.
(42) Wild, S. R.; Jones, K. C. *Environ. Pollut.* **1995**, *88*, 91−108.
(43) Schmidt, M. W. I.; Skjemstad, J. O.; Czimczik, C. I.; Glaser, B.; Prentice, K. M.; Gelinas, Y.; Kuhlbusch, T. A. J. *Global Biogeochem. Cycles* **2001**, *15*, 163−167.
(44) Seinfeld, J. H.; Pandis, S. N. *Atmospheric Chemistry and Physics*; John Wiley & Sons: New York, 1998; p 1326.
(45) Eglinton, T. I.; Eglinton, G.; Dupont, L.; Sholkovitz, E. R.; Montluçon, D.; Reddy, C. M. *Geochem. Geophys. Geosyst.* **2002**, 10.1029/2001/GC000269.
(46) Brunciak, P. A.; Dachs, J.; Gigliotti, C. L.; Nelson, E. D.; Eisenreich, S. J. *Atmos. Environ.* **2001**, *35*, 3325−3339.
(47) Harner, T.; Bidleman, T. F. *Environ. Sci. Technol.* **1998**, *32*, 1494−1502.
(48) Bamford, H. A.; Poster, D. L.; Backer, J. E. *Environ. Toxicol. Chem.* **1999**, *18*, 1905−1912.
(49) Mackay, D.; Shiu, W. Y.; Ma, K. Ch. *Illustrated Handbook of Physical-Chemical Properties and Environmental Fate for Organic Chemicals*. Volume II: Polynuclear Aromatic Hydrocarbons, Polychlorinated Dioxins, and Benzofurans; Lewis Publishers: Pearl River, NY, 1992.

Received for review July 17, 2002. Revised manuscript received March 24, 2003. Accepted March 25, 2003.

ES0201449